

# Looking through the Pseudo-Scalar Portal into Dark Matter: Novel Mono-Higgs and Mono- $Z$ Signatures at LHC

Jose Miguel No<sup>1,\*</sup>

<sup>1</sup>*Department of Physics and Astronomy, University of Sussex, Brighton BN1 9QH, UK*

(Dated: August 20, 2018)

Mono- $X$  signatures are a powerful collider probe of the nature of dark matter. We show that mono-Higgs and mono- $Z$  may be key signatures of pseudo-scalar portal interactions between dark matter and the SM. We demonstrate this using a simple renormalizable version of the portal, with a Two-Higgs-Doublet-Model as electroweak symmetry breaking sector. Mono- $Z$  and mono-Higgs signatures in this scenario are of resonant type, which constitutes a novel type of dark matter signature at LHC.

The nature of dark matter (DM) is an outstanding mystery at the interface of particle physics and cosmology. The current DM candidate paradigm is the so-called Weakly-Interacting-Massive-Particle (WIMP), a particle whose relic abundance is obtained via thermal freeze-out in the early Universe, and with a mass in the range GeV – TeV, around the scale of electroweak (EW) symmetry breaking  $v = 246$  GeV. WIMP DM is very well-motivated in connection with new physics close to the EW scale (see [1] for a review) and/or the existence of a hidden sector (singlet under the SM gauge group) which interacts with the SM via a portal [2, 3].

A large experimental effort aims to reveal the nature of (WIMP) DM and its interactions with SM particles, either indirectly by measuring the energetic SM particles product of DM annihilations in space, or directly by measuring the scattering of ambient DM from heavy nuclei. Current best experimental limits on the spin-independent DM interaction cross section with nuclei by the Large-Underground-Xenon (LUX) experiment [4] are very strong, and particularly constraining for DM masses in the range 10 – 100 GeV. On the other hand, the experimental limits on spin-dependent DM-nucleon interactions are much less stringent, generically favouring a pseudo-scalar mediator of DM-nucleon interactions (which primarily yields spin-dependent interactions) over a scalar mediator.

Direct/indirect probes of DM are complemented by searches at colliders, where pairs of DM particles could be produced. These escape the detector and manifest themselves as events showing an imbalance in momentum conservation, via the presence of missing transverse momentum  $\cancel{E}_T$  recoiling against a visible final state  $X$ . Searches for events with large  $\cancel{E}_T$  are a major activity at the Large Hadron Collider (LHC) precisely due to their (potential) connection to DM [5].

Searches for DM in  $X + \cancel{E}_T$  channels, referred to as *mono- $X$* , can be classified according to the visible particle(s)  $X$  against which the invisible particles recoil. Experimental studies at Tevatron and LHC have considered cases in which  $X$  is a hadronic jet [6–8], a photon  $\gamma$  [9, 10],  $W$  or  $Z$  bosons [11, 12] and, after the recent discovery of

the Higgs boson [13, 14], have also considered  $X$  to be the 125 GeV Higgs particle  $h$  [15]. Indeed, if DM is linked to the EW scale,  $W$ ,  $Z$  and Higgs boson signatures are natural places to search for it, with mono- $W$ ,  $Z$ ,  $h$  having been recently considered as a paradigm for such potential signatures [16–22].

With the EW symmetry breaking sector being a most natural portal to a hidden sector, it is crucial to identify key probes of such portal interactions with the DM sector. As pseudo-scalar portal interactions are significantly more difficult to probe experimentally via direct DM detection, collider probes constitute a rather unique window into these DM scenarios. In this work I investigate such probes for a renormalizable pseudo-scalar Higgs portal (also known as *Axion Portal*) [23], possible within extensions of the SM scalar sector. I show that novel mono-Higgs and mono- $W$ ,  $Z$  signatures emerge in this context, with very distinct kinematical features from other mono- $X$  scenarios. These signatures constitute a new probe of DM scenarios at LHC, deeply linked to the realization of a non-minimal Higgs sector in Nature.

The letter is organized as follows: In Section I we introduce and discuss the pseudo-scalar portal scenario using a simple realization of a DM scenario in this context. In Section II we analyze the mono-Higgs and mono- $Z$  signatures the portal gives rise to, and discuss their prospects for the 14 TeV run of LHC. We finally outline the implications of these results in Section III.

## I. Dark Matter Through the Pseudo-Scalar Portal

The simplest realization of the pseudo-scalar portal occurs within a Two-Higgs-Doublet-Model (2HDM) extension of the SM [23]. For our purposes, we use in the following a simple embedding of DM into such a picture (see e.g. [24]), and consider dark matter to be a Dirac fermion  $\psi$  with mass  $m_\psi$ , which couples to a real singlet pseudo-scalar mediator state  $a_0$  via

$$V_{\text{dark}} = \frac{m_{a_0}^2}{2} a_0^2 + m_\psi \bar{\psi} \psi + y_\psi a_0 \bar{\psi} i \gamma^5 \psi \quad (1)$$

A renormalizable coupling of  $a_0$  to the visible sector becomes possible by extending the SM Higgs sector to in-

clude two doublets  $H_i = (\phi_i^+, (v_i + h_i + \eta_i)/\sqrt{2})^T$  ( $i = 1, 2$ ),  $v_i$  being the *vev* of the doublets with  $\sqrt{v_1^2 + v_2^2} = v$  and  $v_2/v_1 \equiv \tan\beta$ . The 2HDM scalar potential reads

$$\begin{aligned} V_{2\text{HDM}} = & \mu_1^2 |H_1|^2 + \mu_2^2 |H_2|^2 - \mu^2 [H_1^\dagger H_2 + \text{h.c.}] \\ & + \frac{\lambda_1}{2} |H_1|^4 + \frac{\lambda_2}{2} |H_2|^4 + \lambda_3 |H_1|^2 |H_2|^2 \quad (2) \\ & + \lambda_4 |H_1^\dagger H_2|^2 + \frac{\lambda_5}{2} \left[ (H_1^\dagger H_2)^2 + \text{h.c.} \right] \end{aligned}$$

where we assume Charge-Parity (CP) conservation and a  $\mathcal{Z}_2$  symmetry, softly broken by  $\mu$ . Extending this  $\mathcal{Z}_2$  symmetry to the couplings of the doublets  $H_{1,2}$  to fermions allows to forbid potentially dangerous tree-level flavour changing neutral currents, by forcing each fermion type to couple to one doublet only [25]. In Type-I 2HDM all fermions couple to  $H_2$ , while for Type-II 2HDM up-type quarks couple to  $H_2$  and down-type quarks and leptons couple to  $H_1$ . The pseudo-scalar portal between the visible and hidden sectors occurs via [23, 24]

$$V_{\text{portal}} = i \kappa a_0 H_1^\dagger H_2 + \text{h.c.} \quad (3)$$

The scalar spectrum of the 2HDM contains a charged scalar  $H^\pm = \cos\beta \phi_2^\pm - \sin\beta \phi_1^\pm$  and two neutral CP-even scalars  $h = \cos\alpha h_2 - \sin\alpha h_1$ ,  $H_0 = -\sin\alpha h_2 - \cos\alpha h_1$ . We identify  $h$  with the 125 GeV Higgs state, which is SM-like in the limit  $\beta - \alpha = \pi/2$  (see e.g. [26] for a review of 2HDM). For  $\kappa \neq 0$ , the would-be neutral CP-odd scalar  $A_0 = \cos\beta \eta_2 - \sin\beta \eta_1$  mixes with  $a_0$  through (3), yielding two pseudo-scalar mass eigenstates  $a, A$

$$A = c_\theta A_0 + s_\theta a_0 \quad , \quad a = c_\theta a_0 - s_\theta A_0 \quad (4)$$

with  $c_\theta \equiv \cos\theta$  and  $s_\theta \equiv \sin\theta$ . We consider in the following the case in which the singlet-like mediator  $a$  is lighter than  $A$  ( $m_A > m_a$ ), and  $m_a > 2m_\psi$  such that the decay  $a \rightarrow \bar{\psi}\psi$  is possible. In terms of the mass eigenstates, the interactions (1) and (3) become

$$\begin{aligned} V_{\text{dark}} \supset & y_\psi (c_\theta a + s_\theta A) \bar{\psi} i \gamma^5 \psi \\ V_{\text{portal}} = & \frac{(m_A^2 - m_a^2) s_{2\theta}}{2v} (c_{\beta-\alpha} H_0 - s_{\beta-\alpha} h) \quad (5) \\ & \times [aA (s_\theta^2 - c_\theta^2) + (a^2 - A^2) s_\theta c_\theta] . \end{aligned}$$

Gauge interactions of the two doublets  $H_i$  yield the relevant interactions  $aZh \propto s_\theta c_{\beta-\alpha}$ ,  $AZh \propto c_\theta c_{\beta-\alpha}$ ,  $aZH_0 \propto s_\theta s_{\beta-\alpha}$ ,  $AZH_0 \propto c_\theta s_{\beta-\alpha}$ ,  $aW^\pm H^\mp \propto s_\theta s_{\beta-\alpha}$ ,  $AW^\pm H^\mp \propto c_\theta s_{\beta-\alpha}$ , while  $V = V_{2\text{HDM}} + V_{\text{dark}} + V_{\text{portal}}$  yields  $aAh \propto s_{4\theta} s_{\beta-\alpha}$ ,  $a\bar{\psi}\psi \propto c_\theta$  and  $A\bar{\psi}\psi \propto s_\theta$ .

Altogether, the interactions above lead to mono- $h$  and mono- $W, Z$  signatures at LHC in various possible ways, which we discuss in detail in the next Section. In particular, for  $m_A > m_h + m_a$ ,  $m_{H_0} > m_Z + m_a$ ,  $m_{H^\pm} > m_{W^\pm} + m_a$ , this scenario yields a novel signature: “resonant mono- $h, W, Z$ ” respectively via the processes  $pp \rightarrow A \rightarrow h a$ ,  $pp \rightarrow H_0 \rightarrow Z a$ ,  $pp \rightarrow H^\pm \rightarrow W^\pm a$ , with the mediator  $a$  subsequently decaying into DM.

## II. Mono-Higgs and Mono- $W, Z$ Signatures at LHC

As outlined above, in these scenarios there are two different kinds of processes which, through the production of  $X + \bar{\psi}\psi$  ( $X = W, Z, h$ ), lead to mono- $X$  signatures at LHC. Focusing on mono-Higgs for the purpose of illustration, there exist contributions from  $pp(\bar{q}q) \rightarrow Z^* \rightarrow h a$  ( $a \rightarrow \bar{\psi}\psi$ ) and  $pp(gg) \rightarrow A \rightarrow h a$  ( $a \rightarrow \bar{\psi}\psi$ ).

The former is kinematically similar to mono- $h$  signatures in other scenarios [20–22], which are generically suppressed either by the presence of an off-shell or very massive particle in the s-channel. Together with the momentum transfer being cut-off by the parton distribution functions (PDFs), this leads to very small mono-Higgs cross sections, making a mono- $h$  signature difficult to probe at the 14 TeV run of LHC even with a large integrated luminosity, if it solely arises from this type of contribution.

In contrast, for  $m_A > m_h + m_a$  the kinematics of the latter process is very different, due to  $A$  being resonantly produced. In this case, the 4-momentum of  $h$  and  $a$  is kinematically fixed, and  $\cancel{E}_T$  is bounded from above by

$$\cancel{E}_T^{\text{max}} = \frac{1}{2m_A} \sqrt{(m_A^2 - m_h^2 - m_a^2)^2 - 4m_h^2 m_a^2} . \quad (6)$$

The  $\cancel{E}_T$  distribution from this process is a steeply rising function with a sharp cut-off at  $\cancel{E}_T^{\text{max}}$ , a very distinct feature of these scenarios. At the same time, this contribution to mono- $h$  is resonantly enhanced *w.r.t* the former one, generically yielding a much larger cross section. Furthermore, it is important to stress that in this scenario the resonant contribution is proportional to  $s_{\beta-\alpha}^2$  and thus maximal in the 2HDM alignment limit of a SM-like Higgs  $h$  (as favoured by ATLAS and CMS analyses), whereas the off-shell contribution is proportional to  $c_{\beta-\alpha}^2$ , vanishing in that limit.

Before we continue, let us briefly comment on the fact that such resonant mono- $h$  signatures may also occur in a pure 2HDM through the process  $pp(gg) \rightarrow A \rightarrow h Z$  ( $Z \rightarrow \nu\nu$ ). We stress that the phenomenology in the presence of the pseudo-scalar portal to DM is radically different from that of the pure 2HDM. First, contrary to the case of the DM portal, the interaction yielding a mono- $h$  signature in the 2HDM vanishes for a SM-like Higgs  $h$ , as discussed above. Second and most important, for a pure 2HDM the same process with  $Z \rightarrow \ell\ell$  is a much more sensitive probe of the existence of  $A$  than the mono- $h$  signature. This constitutes a generic, crucial way of disentangling a resonant  $X + \cancel{E}_T$  signature where  $\cancel{E}_T$  originates in a dark sector (e.g.  $a \rightarrow \bar{\psi}\psi$ ) from that where the  $\cancel{E}_T$  comes from  $Z \rightarrow \nu\nu$ , as the latter will have to be accompanied by a much more sensitive  $Z \rightarrow \ell\ell$  counterpart, while the former will not.

For our phenomenological analysis, we choose a Type II 2HDM benchmark  $t_\beta = 3$ ,  $c_{\beta-\alpha} = 0.05$  (close to the 2HDM alignment limit) with  $s_\theta = 0.3$ , corresponding

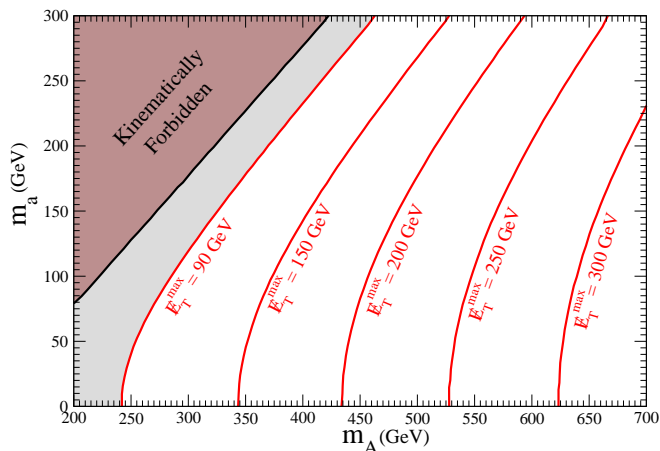


FIG. 1. Value of  $E_T^{\max}$  from (6) for resonant mono- $h$  in the  $(m_A, m_a)$  plane. In the solid-brown region the decay  $A \rightarrow ha$  is kinematically forbidden. The grey region lies below the event selection of [15]. A similar Figure may be obtained in the plane  $(m_{H_0}, m_a)$  for resonant mono- $Z$ .

to a moderate mixing between the visible and dark sectors, and  $y_\psi = 0.2$ . For the mediator and DM masses we choose respectively  $m_a = 80$  GeV,  $m_\psi = 30$  GeV. The DM annihilation cross section in this case is of order needed for a correct DM relic density [24], and we find that for  $m_a, m_\psi$  masses in this ballpark,  $a \rightarrow \bar{\psi}\psi$  yields the dominant branching fraction for  $y_\psi \gtrsim 0.02$ , and  $\text{BR}(a \rightarrow \bar{\psi}\psi) > 0.99$  for  $y_\psi \gtrsim 0.1$ . We take for simplicity  $m_{H^\pm} = m_{H_0} = m_A$ , verifying that it satisfies EW precision observable constraints, and for each value of  $m_A$  we adjust  $\mu$  in (2) to be within the region compatible with vacuum stability, perturbativity and unitarity.

In the following, taking as benchmark values  $m_{H_0} = m_A = 300, 500, 700$  GeV, which we denote respectively as benchmarks A, B, C, we discuss the existing bounds from the 8 TeV LHC run and explore the 14 TeV LHC run prospects for *resonant mono- $h, Z$* .

### Mono-Higgs

Current ATLAS and CMS mono- $h$  searches focus on the  $h \rightarrow \gamma\gamma$  decay of the 125 GeV Higgs boson. For our analysis we use the selection criteria from the LHC 8 TeV run data analysis by ATLAS [15], which selects events with two photons with leading (subleading) transverse momentum  $P_T^\gamma > 35$  (25) GeV, rapidity  $|\eta^\gamma| < 2.37$  and in the invariant mass window  $m_{\gamma\gamma} \in [105, 160]$  GeV. In addition, the photon pair is required to have been produced in association with a sizable amount of missing transverse momentum,  $\cancel{E}_T > 90$  GeV, and such that  $P_T^{\gamma\gamma} > 90$  GeV (to suppress background events where  $\cancel{E}_T$  is caused by mismeasurement of identified physical objects). ATLAS yields a 95 % C.L. upper bound on the cross section of 0.70 fb, while our 8 TeV signal samples for  $m_A = 300, 500, 700$  GeV generated with

MADGRAPH5\_AMC@NLO [27, 28] respectively yield, after selection cuts, 0.143 fb, 0.043 fb and 0.011 fb, including next-to-leading-order (NLO) QCD effects computed using SUSHI [31].

In Figure 1 we show the value of  $E_T^{\max}$  for resonant mono- $h$  in the  $(m_A, m_a)$  plane, which highlights the fact that, while current searches are not sensitive to  $m_A \lesssim 250$  GeV (as  $E_T^{\max} < 90$  GeV), the value of  $E_T^{\max}$  rapidly increases with  $m_A$ , making the signature  $pp \rightarrow h\psi\psi$  ( $h \rightarrow \gamma\gamma$ ) promising for masses  $m_A \gtrsim 300$  GeV at the LHC 14 TeV run. For our analysis of resonant mono- $h$  prospects at LHC 14 TeV, we generate our signal and background event samples with MADGRAPH5\_AMC@NLO. These are passed on to PYTHIA [29] for parton showering and hadronization, and then to DELPHES [30] for a detector simulation. The main SM backgrounds are  $Z\gamma\gamma, Z\gamma$ +jets (with a jet being misidentified as a photon, the fake rate being  $P_{j \rightarrow \gamma} \sim 10^{-3}$  [32]) and SM Higgs associated production  $Zh$ , with  $Z \rightarrow \nu\nu$ . Backgrounds with a  $W$  instead of a  $Z$  boson may be suppressed by vetoing extra leptons. NLO cross section values are estimated via  $K$ -factors:  $K \simeq 1.65, 1.3$  respectively for  $Z\gamma\gamma$  and  $Z\gamma$ +jets [33],  $K \simeq 1.3$  for  $Zh$  [34] and  $K \simeq 2.27, 1.8, 1.69$  respectively for our signal benchmarks A, B, C through SUSHI.

	A	B	C	$Zh$	$Z\gamma\gamma$	$Z\gamma j$
Event selection	249	56	16	51	517	157
$m_{\gamma\gamma} \in [120, 130]$ GeV	161	26	6	34	97	32
$\cancel{E}_T, P_T^{\gamma\gamma} > 80$ GeV	105	24	5	13	32	12
$\cancel{E}_T, P_T^{\gamma\gamma} > 180$ GeV	4	15	4	2	3	2
$\cancel{E}_T, P_T^{\gamma\gamma} > 280$ GeV	< 0.1	2	3	0.4	0.5	0.5

TABLE I. Expected number of events after event selection (see text for details) and signal region cuts for mono- $h$  with  $h \rightarrow \gamma\gamma$ , for LHC 14 TeV with  $\mathcal{L} = 300 \text{ fb}^{-1}$ . Signal benchmarks A, B, C are described in Section II.

In Table I we show the expected signal and background events for LHC at 14 TeV with an integrated luminosity  $\mathcal{L} = 300 \text{ fb}^{-1}$ , after event selection and in the signal region. Event selection requirements for the two photon candidates follow [15] and are described above, dropping the  $\cancel{E}_T > 90$  GeV cut. We subsequently define the signal region via  $m_{\gamma\gamma} \in [120, 130]$  GeV and  $\cancel{E}_T, P_T^{\gamma\gamma} > 80$  GeV, 180 GeV, 280 GeV respectively to maximize the sensitivity to benchmarks A, B, C. The  $\cancel{E}_T$  distribution for the three signal benchmarks and main backgrounds before applying this last cut is shown in Figure 2 (LEFT). From Table I, we see that, upon neglecting systematic uncertainties, an approximate significance  $S/\sqrt{S+B} \sim 7.9, 3.2, 1.5$  is obtained in the signal region respectively for benchmarks A, B, C and  $\mathcal{L} = 300 \text{ fb}^{-1}$ .

### Mono-Z

The recent ATLAS search [12] constraints mono- $Z$  signatures with  $Z \rightarrow \ell^+\ell^-$  using the available LHC 8 TeV

run data. Their analysis selects events with two opposite sign (opposite charges) electrons/muons in the invariant mass window  $m_{\ell\ell} \in [76, 106]$  GeV, with  $P_T^\ell > 20$  GeV and rapidity  $|\eta^\ell| < 2.5$  (2.47) for muons (electrons). The rapidity of the di-lepton system has to satisfy  $|\eta^{\ell\ell}| < 2.5$ , and event selection further requires

$$\Delta\phi(\vec{E}_T, \vec{P}_T^{\ell\ell}) > 2.5, \quad |P_T^{\ell\ell} - E_T|/P_T^{\ell\ell} < 0.5. \quad (7)$$

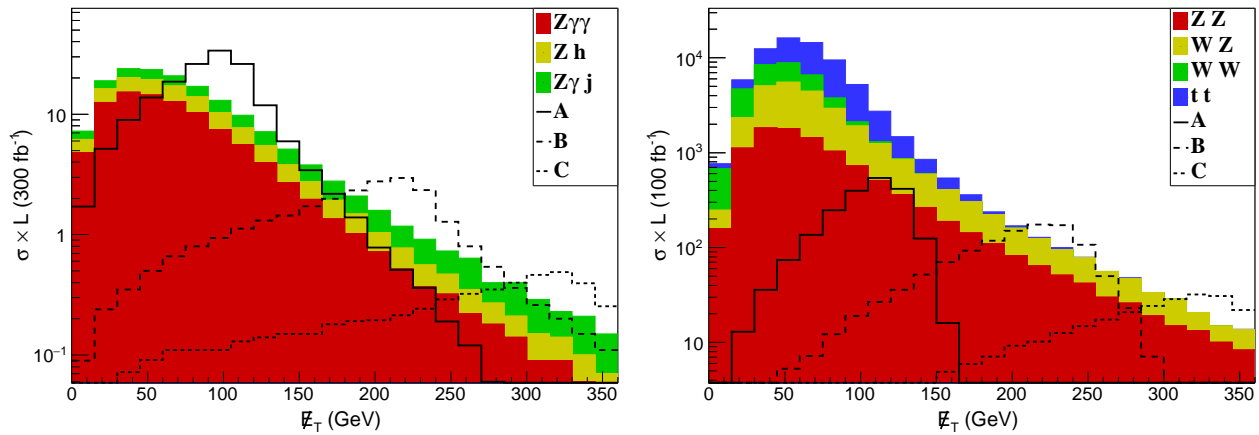


FIG. 2. LEFT:  $E_T$  distribution for mono- $h$  signal benchmarks A (solid black), B (dashed black), C (fine-dashed black) and background processes  $Z\gamma\gamma$  (red),  $Zh$  (yellow) and  $Z\gamma j$  (green), yielding  $E_T + \gamma\gamma$ , after event selection (see text for details) and for  $m_{\gamma\gamma} \in [120, 130]$  GeV. RIGHT:  $E_T$  distribution for mono- $Z$  signal benchmarks A, B, C and background processes  $ZZ$  (red),  $WZ$  (yellow),  $WW$  (green) and  $t\bar{t}$  (blue), yielding  $E_T + \ell^+\ell^-$ , after event selection (see text for details). In both cases, backgrounds are stacked on top of each other while signals are not, with bins being 15 GeV wide and normalized to show the number of events per bin.

For our resonant mono- $Z$  analysis at LHC 14 TeV, we follow a similar procedure to the one described for the mono- $h$  case in the previous section, using MADGRAPH5\_AMC@NLO, PYTHIA and DELPHES for our signal  $pp \rightarrow Za$  ( $Z \rightarrow \ell^+\ell^-$ ,  $a \rightarrow \psi\psi$ ) and background event samples. The SM irreducible backgrounds are  $ZZ \rightarrow \ell^+\ell^- \nu\bar{\nu}$  and  $WW \rightarrow \ell^+\nu \ell^-\bar{\nu}$ , while  $WZ \rightarrow \ell\nu \ell^+\ell^-$  and  $t\bar{t} \rightarrow b\ell^+\nu \bar{b}\ell^-\bar{\nu}$  are the most important reducible backgrounds. NLO cross sections are estimated via  $K$ -factors:  $K \simeq 1.2, 1.79, 1.68$  respectively for  $ZZ, WZ$  and  $WW$  [35],  $K \simeq 1.5$  for  $t\bar{t}$  [34] and  $K \simeq 2.36, 1.88, 1.75$  respectively for our signal benchmarks A, B, C via SUSHI. Our event selection follows [12] and is discussed above, and we define three signal regions  $E_T, P_T^{\gamma\gamma} > 90$  GeV, 190 GeV, 290 GeV to respectively maximise sensitivity to benchmarks A, B, C.

In Table II we show the expected signal and background events for LHC at 14 TeV with an integrated luminosity  $\mathcal{L} = 100 \text{ fb}^{-1}$ , after event selection and in the various signal regions. Neglecting systematic un-

Four signal regions are defined, corresponding respectively to  $E_T > 150$  GeV, 250 GeV, 350 GeV and 450 GeV. The ATLAS analysis yields respective 95 % C.L. observed upper bound on the cross section of 2.7 fb, 0.57 fb, 0.27 fb and 0.26 fb. Our three signal benchmark scenarios, A, B, C, satisfy these bounds, and as we show in the following they are very promising for the 14 TeV run of LHC.

certainties, an approximate significance  $S/\sqrt{S+B} \sim 12.8, 18.7, 9.2$  is obtained in the respective optimal signal region for benchmarks A, B, C. In Figure 2 (RIGHT), we show the  $E_T$  distribution for signal and background after event selection.

	A	B	C	ZZ	WW	WZ	$t\bar{t}$
Event selection	2009	1130	282	10100	12670	16680	32060
$E_T > 90$ GeV	1500	1105	279	2660	253	3530	5660
$E_T > 190$ GeV	4.5	733	254	414	< 0.1	357	30
$E_T > 290$ GeV	1.5	11	158	81	-	57	< 0.1

TABLE II. Expected number of events after event selection (see text for details) and in the signal region for mono- $Z$  with  $Z \rightarrow \ell^+\ell^-$ , for LHC 14 TeV with  $\mathcal{L} = 100 \text{ fb}^{-1}$ . Signal benchmarks A, B, C are described in Section II.

Finally, although not discussed in his work, resonant mono- $W$  signatures are also possible in this setup, but the suppressed production of  $H^\pm$  compared to  $A/H_0$  makes them much less promising.

### III. Discussion and Outlook

The analysis of the previous Section shows that resonant mono-Higgs and mono- $Z$  are promising signatures for the 14 TeV run of LHC with  $\mathcal{L} = 100 - 300 \text{ fb}^{-1}$ , with mono- $Z$  in particular being a very sensitive probe of pseudo-scalar portal scenarios like the one discussed here. Moreover, not only these signatures constitute a window into the DM sector, but are also potential discovery modes for the heavy states of the non-minimal scalar sector (here  $A, H_0$ ), as their “usual” decay modes (e.g. in a pure 2HDM) will get suppressed by the presence of the new decay channels into the dark sector.

Finally, there are other possible avenues for exploring these pseudo-scalar portal scenarios, like mono-jet searches on  $pp(gg) > aj(a \rightarrow \bar{\psi}\psi)$ , which we do not explore here, but will most certainly be complementary to the ones introduced in this work. One other aspect I have not explored is the possibility of a light  $a$  state, such that  $m_h - m_Z > m_a > 2m_\psi$ . The exotic Higgs decay  $h \rightarrow Za \rightarrow \ell^+\ell^-\bar{\psi}\psi$  is an interesting signature of such scenarios, and will be studied elsewhere.

To conclude, I have shown that, for DM scenarios with a pseudo-scalar mediator between the visible and DM sectors, novel potential collider signatures emerge in the form of *resonant mono- $h, Z$* . These constitute a new probe of DM scenarios at LHC, very promising for the 14 TeV run, and would also point to the realization of a non-minimal Higgs sector in Nature.

### Acknowledgements

I want to thank the organizers of the Les Houches 2015 Workshop “Physics at TeV Colliders” where this work begun, and also Ken Mimasu, Veronica Sanz, Seyda Ipek and Belen Lopez-Laguna for very useful discussions. J.M.N. is supported by the People Programme (Marie Curie Actions) of the European Union Seventh Framework Programme (FP7/2007-2013) under REA grant agreement PIEF-GA-2013-625809.

---

\* j.m.no@sussex.ac.uk

- [1] G. Bertone, D. Hooper and J. Silk, Phys. Rept. **405**, 279 (2005) [hep-ph/0404175].
- [2] R. Schabinger and J. D. Wells, Phys. Rev. D **72**, 093007 (2005) [hep-ph/0509209].
- [3] B. Patt and F. Wilczek, hep-ph/0605188.
- [4] D. S. Akerib *et al.* [LUX Collaboration], Phys. Rev. Lett. **112**, 091303 (2014) [arXiv:1310.8214 [astro-ph.CO]].
- [5] D. E. Morrissey, T. Plehn and T. M. P. Tait, Phys. Rept. **515**, 1 (2012) [arXiv:0912.3259 [hep-ph]].
- [6] T. Aaltonen *et al.* [CDF Collaboration], Phys. Rev. Lett. **108**, 211804 (2012) [arXiv:1203.0742 [hep-ex]].
- [7] V. Khachatryan *et al.* [CMS Collaboration], Eur. Phys. J. C **75**, no. 5, 235 (2015) [arXiv:1408.3583 [hep-ex]].
- [8] G. Aad *et al.* [ATLAS Collaboration], Eur. Phys. J. C **75**, no. 7, 299 (2015) [arXiv:1502.01518 [hep-ex]].
- [9] S. Chatrchyan *et al.* [CMS Collaboration], Phys. Rev. Lett. **108**, 261803 (2012) [arXiv:1204.0821 [hep-ex]].
- [10] G. Aad *et al.* [ATLAS Collaboration], Phys. Rev. Lett. **110**, no. 1, 011802 (2013) [arXiv:1209.4625 [hep-ex]].
- [11] G. Aad *et al.* [ATLAS Collaboration], Phys. Rev. Lett. **112**, no. 4, 041802 (2014) [arXiv:1309.4017 [hep-ex]].
- [12] G. Aad *et al.* [ATLAS Collaboration], Phys. Rev. D **90**, no. 1, 012004 (2014) [arXiv:1404.0051 [hep-ex]].
- [13] G. Aad *et al.* [ATLAS Collaboration], Phys. Lett. B **716** (2012) 1 [arXiv:1207.7214 [hep-ex]].
- [14] S. Chatrchyan *et al.* [CMS Collaboration], Phys. Lett. B **716** (2012) 30 [arXiv:1207.7235 [hep-ex]].
- [15] G. Aad *et al.* [ATLAS Collaboration], arXiv:1506.01081 [hep-ex].
- [16] F. J. Petriello, S. Quackenbush and K. M. Zurek, Phys. Rev. D **77**, 115020 (2008) [arXiv:0803.4005 [hep-ph]].
- [17] Y. Bai and T. M. P. Tait, Phys. Lett. B **723**, 384 (2013) [arXiv:1208.4361 [hep-ph]].
- [18] N. F. Bell, J. B. Dent, A. J. Galea, T. D. Jacques, L. M. Krauss and T. J. Weiler, Phys. Rev. D **86**, 096011 (2012) [arXiv:1209.0231 [hep-ph]].
- [19] L. M. Carpenter, A. Nelson, C. Shimmin, T. M. P. Tait and D. Whiteson, Phys. Rev. D **87**, no. 7, 074005 (2013) [arXiv:1212.3352 [hep-ex]].
- [20] A. A. Petrov and W. Shepherd, Phys. Lett. B **730**, 178 (2014) [arXiv:1311.1511 [hep-ph]].
- [21] L. Carpenter, A. DiFranzo, M. Mulhearn, C. Shimmin, S. Tulin and D. Whiteson, Phys. Rev. D **89**, no. 7, 075017 (2014) [arXiv:1312.2592 [hep-ph]].
- [22] A. Berlin, T. Lin and L. T. Wang, JHEP **1406**, 078 (2014) [arXiv:1402.7074 [hep-ph]].
- [23] Y. Nomura and J. Thaler, Phys. Rev. D **79** (2009) 075008 [arXiv:0810.5397 [hep-ph]].
- [24] S. Ipek, D. McKeen and A. E. Nelson, Phys. Rev. D **90** (2014) 5, 055021 [arXiv:1404.3716 [hep-ph]].
- [25] S. L. Glashow and S. Weinberg, Phys. Rev. D **15**, 1958 (1977).
- [26] G. C. Branco, P. M. Ferreira, L. Lavoura, M. N. Rebelo, M. Sher and J. P. Silva, Phys. Rept. **516**, 1 (2012) [arXiv:1106.0034 [hep-ph]].
- [27] J. Alwall, M. Herquet, F. Maltoni, O. Mattelaer and T. Stelzer, JHEP **1106**, 128 (2011) [arXiv:1106.0522 [hep-ph]].
- [28] J. Alwall, R. Frederix, S. Frixione, V. Hirschi, F. Maltoni, O. Mattelaer, H. -S. Shao and T. Stelzer *et al.*, arXiv:1405.0301 [hep-ph].
- [29] T. Sjostrand, S. Mrenna and P. Z. Skands, Comput. Phys. Commun. **178**, 852 (2008) [arXiv:0710.3820 [hep-ph]].
- [30] J. de Favereau *et al.* [DELPHES 3 Collaboration], JHEP **1402**, 057 (2014) [arXiv:1307.6346 [hep-ex]].
- [31] R. V. Harlander, S. Liebler and H. Mantler, Computer Physics Communications **184**, 1605 (2013) [arXiv:1212.3249 [hep-ph]].
- [32] J. Lilley, CERN-THESIS-2011-013.
- [33] J. M. Campbell, H. B. Hartanto and C. Williams, JHEP **1211**, 162 (2012) [arXiv:1208.0566 [hep-ph]].
- [34] F. Maltoni, K. Mawatari and M. Zaro, Eur. Phys. J. C **74**, no. 1, 2710 (2014) [arXiv:1311.1829 [hep-ph]].
- [35] J. Ohnemus, Phys. Rev. D **50**, 1931 (1994) [hep-ph/9403331].
- [36] M. L. Mangano, P. Nason and G. Ridolfi, Nucl. Phys. B **373**, 295 (1992); G. Bevilacqua, M. Czakon, A. van Hameren, C. G. Papadopoulos and M. Worek, JHEP **1102**, 083 (2011) [arXiv:1012.4230 [hep-ph]].